Progress In Electromagnetics Research C, Vol. 19, 25–35, 2011

PRINTED LOOP ANTENNA INTEGRATED INTO A COMPACT, OUTDOOR WLAN ACCESS POINT WITH DUAL-POLARIZED RADIATION

S.-W. Su

Network Access Strategic Business Unit
Lite-On Technology Corporation, Taipei County 23585, Taiwan

Abstract—A printed loop antenna for integration into a compact, outdoor WLAN access point (AP) is presented. The loop design has a one-wavelength, resonant structure with respect to the center operating frequency of the 2.4 GHz band and is formed on a 1.6-mm thick FR4 substrate. The antenna substrate is further stacked above a system printed circuit board (PCB) of an outdoor AP by a small distance. In this study, the proposed design integrates the system PCB serving as an efficient reflector for the loop into an internal AP antenna solution. The results showed that by feeding the proposed square loop at one corner and adding the tuning portion at the diagonal corner, the dual-polarized radiation in the two major planes and good impedance matching over the band can be attained. High gain, directional radiation patterns were also obtained.

1. INTRODUCTION

Antennas with dual-polarized radiation properties have been very attractive to base- station antenna designs for mobile communications [1] and WLAN [2–4] applications. Particularly, the dual-polarized antennas are advantageous for combating the complex propagation of the transmit/receive waves in the WLAN environment. In addition, the polarization sensitivity of the antenna is reduced by using the dual-polarized antennas. These kinds of antenna designs usually include two antenna ports with various feed techniques, for instance, the use of hybrid feeds as elaborated in [1] to decouple the two antenna ports. As for the single-feed, dual-polarized antennas, the related studies are very

Received 26 October 2010, Accepted 9 December 2010, Scheduled 24 December 2010
Corresponding author: Saou-Wen Su (stephen.su@liteon.com).

scant for WLAN access point (AP) [3]. It is interesting to mention that these antennas are mostly microstrip or patch antennas due largely to their attractive features of low profile, light weight, and high antenna gain. However, the microstrip and patch antennas are well known to operate as a half-wavelength, resonant structure [5] and may partly occupy limited design space. In this Letter, we demonstrate a simple and promising design concept that makes use of a one-wavelength loop antenna to be integrated into a compact, outdoor WLAN AP for dual-polarization operation in the AP's two major planes. Substantially different from the microstrip and patch antenna structure (a top patch placed above a ground plane with feeding pin located therein between), the proposed design does not require an antenna ground and treats the AP's system ground as a reflector. Moreover, because the proposed loop is a self-balanced structure, the antenna input matching is expected to be less affected when the loop is placed above the system printed circuit board (PCB) with various location D [see Fig. 1(c)]. Notice that this kind of the outdoor AP has a low profile and robust enclosure, which is often in the shape of a rectangular box [6].

The proposed design comprises a one-wavelength loop and a tuning portion, all printed on a low-cost FR4 substrate within the boundary of a system PCB with size of 70 mm $\times$ 100 mm of an outdoor AP. The antenna is stacked above the system PCB by an air separation distance. In this case, the design integrates the system PCB as an efficient reflector for the loop antenna to achieve directional radiation patterns. The loop antenna is square in shape and fed at one corner; the tuning portion is placed opposite the antenna feed at the diagonal corner. With this corner-feed structure, the current vectors on every adjacent sides of the square loop are not only orthogonal to each other but also in the same direction (see Fig. 9). Accordingly, the dual-polarization radiation patterns are realized in the AP's two major planes (see Fig. 6), which is substantially different, compared with the good polarization purity for the corresponding reference loop (see Fig. 6). The antenna can also serve the 1×1 ($T_x \times R_x$) configuration for MIMO operation with an external duplexer required and used in the RF circuitry.

2. ANTENNA CONFIGURATION AND DESIGN CONSIDERATION

Figure 1(a) demonstrates an example of a possible, compact outdoor AP including the proposed design. The proposed antenna is stacked above a system PCB of an outdoor AP by an air separation distance. A sectional view of the design is shown in Fig. 1(b). The system ground

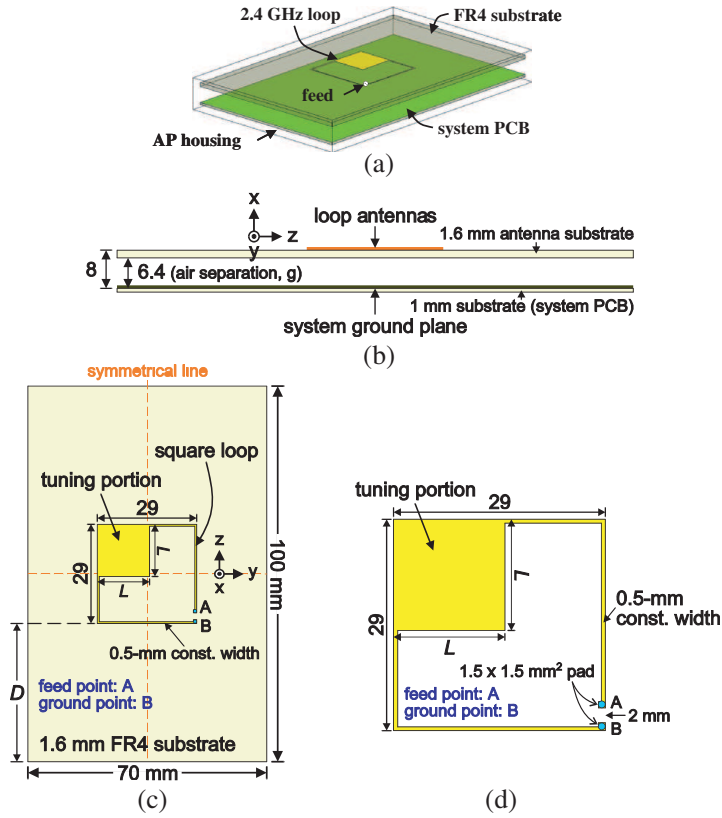

Figure 1. (a) Perspective drawing of the proposed printed loop antenna integrated into a compact outdoor AP. (b) Sectional view of the proposed design backed by a system PCB of an AP. (c) Geometry of the proposed loop antenna formed on a low-cost FR4 substrate. (d) Detailed dimensions of the loop antenna.

of the PCB in this study can be considered an efficient reflector for the antenna, giving more radiation strength in the $+x$ direction. The separation distance of 6.4 mm allows small electric components in the circuitry to be set on the PCB layer that faces the antenna. The antenna substrate is a standard, 1.6-mm thick FR4 substrate. In this case, the antenna is set 8 mm high above the AP system ground.

Figure 1(c) shows the geometry of the proposed loop antenna formed on the FR4 substrate within the boundary of the system PCB with the dimensions 70 mm $\times$ 100 mm. For manufacture-cost concern, the antenna substrate can be reduced to only the necessary area of the

square loop, which occupies the size of 29 mm × 29 mm. The loop is placed in the center of the antenna substrate with a distance D from the bottom side of the substrate. Further detailed dimensions for the loop antenna are presented in Fig. 1(d). The antenna is designed to operate in the 2.4 GHz band, has a constant strip width of 0.5 mm, and comprises a square tuning portion with a side length L. The feed gap across feed point A and ground point B is set to 2 mm for better impedance matching and ease of cable soldering. Notice that two widened pads of size 1.5 mm × 1.5 mm were added to accommodate the outer conductor of the mini-coaxial cable that has an overall diameter of 1.13 mm (see Fig. 1(b) in [7]). The loop antenna in this design has an average resonant path of 105 mm, which is about one wavelength at 2442 MHz, the center operating frequency of the 2.4 GHz band. Thus, the loop is in one-wavelength (balanced) mode, which induced less surface currents on the antenna/system ground [8], compared with the PIFA-like, short-circuited (unbalanced) AP antennas [9, 10], thereby making the ground plane even a better reflector here. For practical, industrial applications, the antenna coaxial cable is further connected to the 2.4 GHz WLAN module on the system PCB. For unbalanced antennas, there also exist strong surface currents on the cable, such that the add-on chokes are usually employed close to the connector side on the system PCB. Without the chokes, the surface currents can flow through the cable, the grounding portion of the connector, and arrive at the system PCB. By using a self-balanced antenna, less surface currents on the coaxial cable are obtained, which in turn leads to less surface currents on the system ground plane. Notice that compared with the 2.4-GHz AP patch antenna with similar antenna ground size in [11], the area of the proposed loop only occupies about one quarter of that of the radiating patch antenna.

Figure 2. Photo of a constructed prototype.

The tuning portion in this design is used to well match the loop antenna, reduce the larger resistance toward 50 Ω, and make the surface-current distribution less dense around the corner (see Fig. 9). However, the resonant path associated with the tuning portion area is also noticeably decreased, which could be a disadvantage to antenna minimization. A photo of a constructed prototype is shown in Fig. 2. As can be seen, the loop antenna is located in the center of the antenna substrate and fed by utilizing a short mini-coaxial cable of length about 60 mm across the feed gap. For practical, industrial applications, this coaxial cable is further connected to the 2.4 GHz WLAN module on the system circuit board through a pair of I-PEX connectors.

3. RESULTS AND DISCUSSION

Based on the design and dimensions thereof described in Fig. 1, a design prototype as shown in Fig. 2 was first constructed and measured. Fig. 3 shows the measured and simulated return loss. It is first noticed that the experimental data compare favorably with the simulation results, which were calculated using the finite element method (FEM). The measured impedance matching over the 2.4 GHz band is all below VSWR of 2, which meets the matching and bandwidth specification for the 2.4 GHz WLAN operation. Some discrepancies were found due largely to PCB manufacture tolerance and the effects of the coaxial cables in the experiments. Further, when there was no tuning portion (that is, the loop with $L = 0.5$ mm), not only the operating frequencies of the antenna decreased from about 2.44 GHz to 2.04 GHz, but the input matching deteriorated rapidly (see comparison in Fig. 4). This

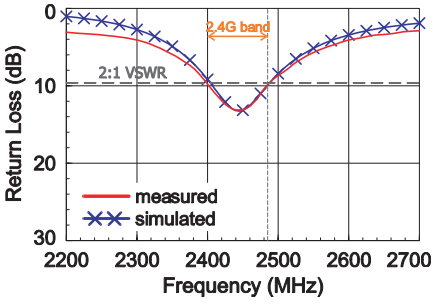

Figure 3. Measured and simulated return loss; $D = 35.5$ mm, $L = 15$ mm.

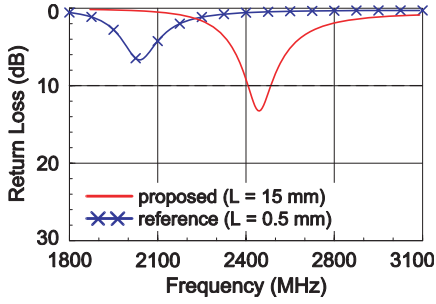

Figure 4. Simulated return loss for the proposed antenna with ($L = 15$ mm) and without ($L = 0.5$ mm) the tuning portion.

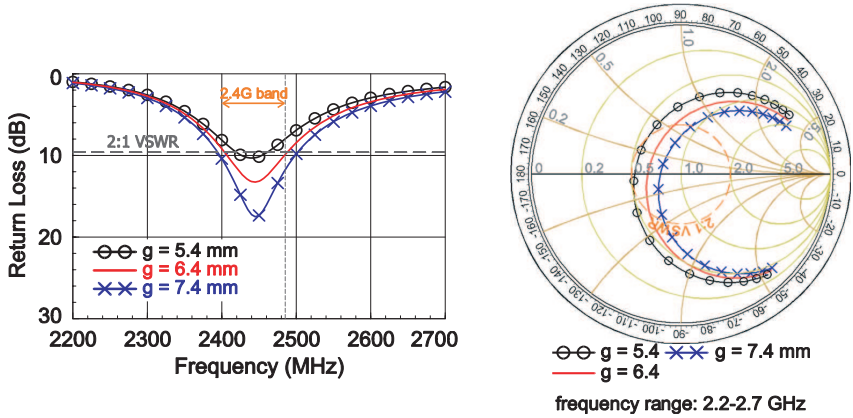

(a) (b)

Figure 5. Simulated (a) return loss and (b) input impedance on the Smith chart as a function of the distance g of the air separation.

behavior indicates that the tuning portion is quite beneficial to good impedance matching but at the same time, can increase the antenna operating frequencies.

Simulation studies of the effects of the air separation distance g on the antenna impedance bandwidth were also conducted. Fig. 5(a) presents the return loss as a function of the distance g. The step of distance 1 mm was taken in analysis. The input-impedance curves on the Smith chart in the frequency range of 2.2–2.7 GHz are separately shown in Fig. 5(b). It is seen that for 2.4 GHz operation, the impedance bandwidth quickly deteriorates with a 1 mm decrease in the separation distance. This is because the central operating frequency of the proposed antenna lies at the x-axis (plotting resistance only) and shifts (to the right) toward the 50 Ω termination as the antenna moves away from the system ground plane [see Fig. 5(b)]. As a general rule of thumb, increasing the air separation leads to better matched operating bands of the antenna. However, it is obvious that a further larger separation distance is neither desired nor practical because the overall size of the AP will be increased.

The radiation characteristics of the proposed design were studied. Fig. 6 shows the far-field, 2-D radiation patterns at 2442 MHz, the center operating frequency of the 2.4 GHz band, in E_θ and E_φ fields for the proposed and the reference antennas. The reference antenna has a side length of 24 mm with the same constant width of 0.5 mm but is symmetrically fed in the center of the bottom side of the loop [see the inset in Fig. 6(b)]. Notice that the x-z and x-y planes

are considered the two major planes mainly because the outdoor AP is usually mounted on the wall or attached to a mast for practical applications. For the proposed antenna in Fig. 6(a), the maximum field strength is in the $+x$ direction with the front-to-back ratio larger than about 15 dB in the x-z and x-y planes. As for the reference antenna, similar radiation properties, in which the peak gain occurs in the normal direction to the substrate and away from the antenna substrate, can be found in Fig. 6(b). But the reference antenna only has constructive current distribution in the horizontal (x-y) plane and thus gains more polarization purity of E_φ fields, in which the cross-polarization level (XPL) is seen to exceed 40 dB. In contrast, the proposed antenna yields dual-polarized radiation with 3-dB XPL range in the elevation (x-z) and the horizontal planes about 147° and 116° respectively. Notice that the 3-dB XPL is defined here for E_θ and E_φ field variations less than 3 dB.

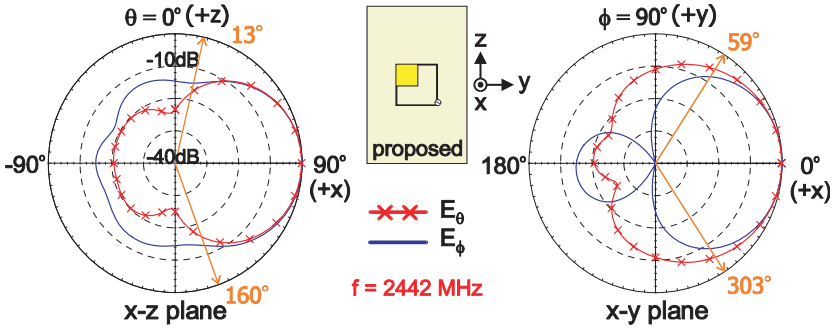

(a)

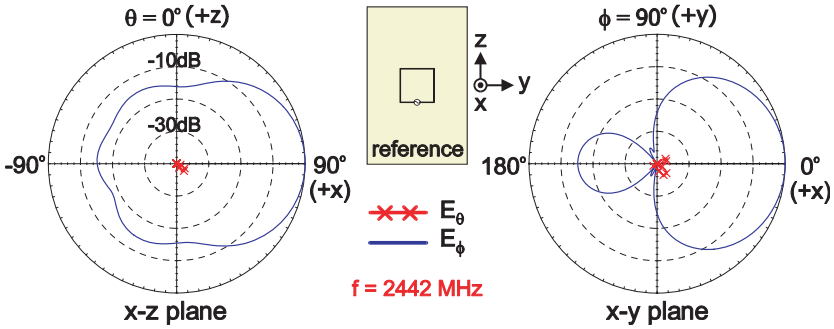

(b)

Figure 6. Simulated 2-D radiation patterns at 2442 MHz: (a) for the proposed antenna studied in Fig. 3; (b) for the reference antenna (symmetrically fed in the center of the bottom side of the square loop).

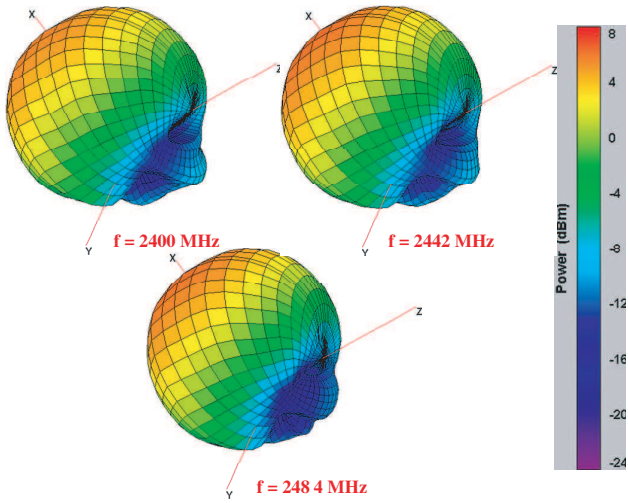

Figure 7. Measured 3-D radiation patterns at 2400, 2442, and 2484 MHz for the proposed antenna studied in Fig. 3.

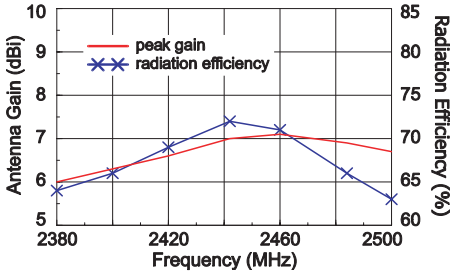

Figure 8. Measured peak antenna gain and radiation efficiency.

Figure 7 plots the measured far-field, 3-D radiation patterns at 2400, 2442, and 2484 MHz in E-total field (combined power of E_θ and E_φ radiation). The measurement was taken by the ETS-Lindgren OTA test system using the great-circle method in a CTIA authorized test laboratory [12]. Compared with other frequencies measured over the band, good consistency in the radiation patterns was also observed. From the results, it is clearly to see high-gain, directional radiation in the $+x$ direction above the y-z plane. The measured peak antenna gain and radiation efficiency for the proposed antenna are presented in Fig. 8. The peak gain in the 2.4 GHz band is at a constant level of about 6.7 dBi with radiation efficiency exceeding 63%. The gain measurement here takes account of the mismatch of the loop antenna,

and thus, the "realized gain" [13] was actually measured in this study. The radiation efficiency was obtained by calculating the total radiated power (TRP) of the antenna under test (AUT) over the 3-D spherical radiation first and then dividing that total amount by the input power of 0 dBm (default value) given to the AUT.

In order to understand the one-wavelength, square-loop structure and its feeding mechanism in relation to the dual-polarized operation, the simulated surface-current distribution on the loop antenna are studied in Fig. 9. The results for the corresponding reference antenna shown in Fig. 6(b) is also presented for comparison. The antennas were excited at the central frequency, 2442 MHz, of the 2.4 GHz band. The currents are plotted in the form of vectors (of an arrow shape) to identify the current nulls, and the thicker the arrow is, the stronger (more magnitude) the current is. First, for both antennas, it can be seen that the currents across the feed gap are out of the phase (currents entering point A and leaving point B). The current vectors of the reference loop along the y axis face in the same direction, while those along the z axis face in the opposite direction. Thus, the E_θ field is cancelled out, and the E_φ field is enhanced, leading to good polarization purity for the reference loop. Second, for the proposed loop, the current nulls and the maximum currents occur at around the diagonal corners of the loop. The current vectors, in this case, on every adjacent sides of the square loop are orthogonal to each other. The current vectors on the two sides of the loop either along the y axis or along the z axis are in the same direction. These suggest that the E_θ and E_φ fields are not only enhanced but also orthogonal to each other, making it possible for the antenna to radiate dual-polarized waves.

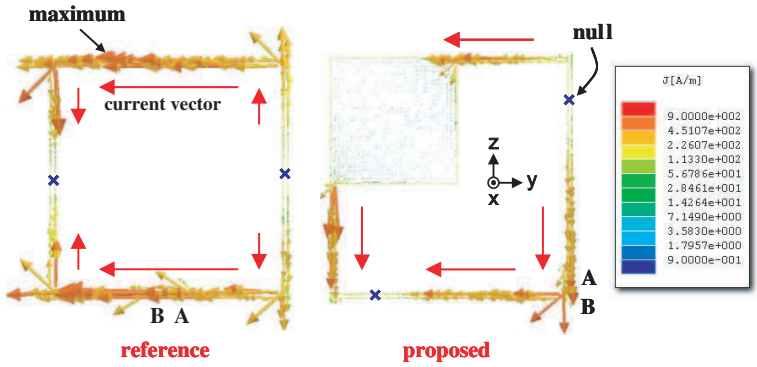

Figure 9. Simulated excited surface currents in the form of vectors at 2442 MHz on the proposed and the reference antennas.

Finally, the studies of the loop antenna located at the top (D = 68 mm) and the bottom (D = 3 mm) side of the antenna substrate were also conducted. The simulated results (not shown for brevity) of the return loss showed that moderate operating-frequency shifting was first noticed with similar impedance matching among due probably to the use of the self-balanced loop structure. This relaxes the proposed design when applying the antenna to a typical, compact outdoor AP with various antenna locations. However, due to the asymmetrical arrangement of the loop with respect to the AP system PCB (the reflector), the quality of the dual-polarization operation is affected, especially in the x-z plane. Also from the simulated results, the 3-dB XPL range was reduced from 147° (proposed in the center) to 64° (at top) and 50° (at bottom) in the elevation (x-z) planes but increased from 116° (proposed in the center) to 127° (at top) and 124° (at bottom) in the horizontal (x-y) planes. Despite all the effects, the antenna still provides fair dual-polarized radiation when not located in the center. These results suggest that the proposed design can be applied to a two-loop-antenna system (one loop at top and the other at bottom) for MIMO AP applications in the future studies.

4. CONCLUSION

A printed loop antenna able to operate in the 2.4 GHz WLAN band for internal AP-antenna applications has been proposed and tested. A self-balanced, one-wavelength, square loop antenna was employed and printed on a FR4 substrate with size of 70 mm × 110 mm within the boundary of the system PCB, above which the loop was stacked by a small distance of 6.4 mm. The self-balanced structure allows the loop to be flexibly deployed in the middle or the top/bottom side of the substrate without much affecting operating band and peak gain. In addition, by feeding the square loop at the corner, the current vectors on every adjacent sides of the loop are orthogonal to each other, which, in turn, results in the dual polarization in the AP's two major planes. The 3-dB XPL in the elevation and horizontal planes is respectively about 147° and 116°. Directional radiation with the front-to-back ratio larger than 15 dB and peak antenna gain larger than 7 dBi have been obtained, too. It is also expected that the design is also suitable for MIMO applications when combining multiple proposed antennas.

REFERENCES

1. Wong, K. L., *Planar Antennas for Wireless Communications*, Chap. 4, 173–193, John Wiley & Sons, Inc., New York, 2003.

2. Guo, Y. X. and K. M. Luk, "Dual-polarized dielectric resonator antennas," *IEEE Antennas Propagat.*, Vol. 51, 1120–1124, 2003.
3. See, T. S. P. and Z. N. Chen, "Design of dual-polarization stacked arrays for ISM band applications," *Microwave Opt. Technol. Lett.*, Vol. 38, 142–147, 2003.
4. Chang, F. S., H. T. Chen, K. C. Chaou, and K. L. Wong, "Dual-polarized probe-fed patch antenna with highly decoupled ports for WLAN base station," *IEEE Antennas Propagat. Soc. Int. Symp. Dig.*, 101–109, Monterey, CA, USA, 2004.
5. Kraus, J. D. and R. J. Marhefka, *Antennas: For All Applications*, 3rd Edition, Chap. 9, 322–329, McGraw-Hill, New York, 2003.
6. NanoStation, Ubiquiti Networks, Inc., http://www.ubnt.com/products/nsm.php.
7. Su, S. W., T. C. Hong, and F. S. Chang, "Very compact coupled-fed loop antenna for 2.4 GHz WLAN applications," *Microwave Opt. Technol. Lett.*, Vol. 52, 1883–1887, 2010.
8. Morishita, H., Y. Kim, and K. Fujimoto, "Design concept of antennas for small mobile terminals and the future perspective," *IEEE Antennas Propagat. Mag.*, Vol. 44, 30–34, 2002.
9. Chou, J. H. and S. W. Su, "Internal wideband monopole antenna for MIMO access-point applications in the WLAN/WiMAX bands," *Microwave Opt. Technol. Lett.*, Vol. 50, 1146–1148, 2008.
10. Su, S. W., "Very-low-profile monopole antennas for concurrent 2.4- and 5-GHz WLAN access-point applications," *Microwave Opt. Technol. Lett.*, Vol. 51, 2614–2617, 2009.
11. Chang, F. S., Y. T. Liu and S. W. Su, "A probe-fed patch antenna with a step-shaped ground plane for 2.4 GHz access point," *Microwave Opt. Technol. Lett.*, Vol. 51, 139–141, 2009.
12. CTIA authorized test laboratory, CTIA — The Wireless Association, http://www.ctia.org/business_resources/certification/test_labs/.
13. Volakis, J. L., *Antenna Engineering Handbook*, 4th edition, Chap. 6, 16–19, McGraw-Hill, New York, 2007.